Physics Letters B 753 (2016) 86–90

Contents lists available at ScienceDirect

Physics Letters B

www.elsevier.com/locate/physletb

Electromagnetic properties of neutron-rich nuclei adjacent to the $Z = 50$ shell closure

M. Rejmund [a], A. Navin [a,*], S. Biswas [b], A. Lemasson [a], M. Caamaño [c], E. Clément [a], O. Delaune [a], F. Farget [a], G. de France [a], B. Jacquot [a], P. Van Isacker [a]

[a] GANIL, CEA/DSM – CNRS/IN2P3, Bd Henri Becquerel, BP 55027, F-14076 Caen Cedex 5, France
[b] DNAP, Tata Institute of Fundamental Research, Mumbai 400005, India
[c] USC, Universidad de Santiago de Compostela, E-15706 Santiago de Compostela, Spain

ARTICLE INFO

Article history:
Received 14 September 2015
Received in revised form 10 November 2015
Accepted 24 November 2015
Available online 8 December 2015
Editor: V. Metag

Keywords:
Isotopic identification
Large isospin and high angular momentum
Spin orbit partners
In-Sb isotopes
M1/E2 transitions
Seniority

ABSTRACT

Low-lying high-spin yrast states in the exotic odd–odd isotopes $^{124-128}$Sb ($Z = 51$) and $^{118-128}$In ($Z = 49$), studied for the first time, show a striking difference in their observed γ-ray decay. With a single valence proton particle/hole occupying the $g_{7/2}/g_{9/2}$ spin-orbit partners, dominant electric quadrupole transitions occur in Sb as opposed to magnetic dipole transitions in In. The observed properties are explained on the basis of general principles of symmetry and with large-scale shell-model calculations, and reveal novel aspects of the competition between the neutron–proton interaction and the like-nucleon pairing interaction.

Nuclear magnetic dipole (M1) moments and transitions, having contributions from both neutrons and protons, are especially suited for studying spin and isospin characteristics of nuclei [1]. The magnetic moment μ (or g factor, $gJ = \mu/\mu_N$, where J is the nuclear angular momentum) of a level in an odd-mass nucleus is, in the extreme single-particle limit, given by the Schmidt value [2] that results from the parallel or anti-parallel coupling of the orbital angular momentum ℓ and the spin of the unpaired nucleon. Observed deviations from the Schmidt value have attracted attention since the 1950s [3–5] and their understanding remains an open problem to this day [6–8]. The deviations are attributed mainly to core polarization (coupling to $\lambda^\pi = 1^+$ particle-hole states in spin-orbit partner shells) and to meson exchange currents (modification of the virtual-meson cloud around a nucleon, due to the presence of other nucleons). M1 transitions between short-lived states reflect the resemblance of the wave function of initial and final states, provide information that is complementary to that obtained from magnetic moments, and have played a critical role in unveiling the existence of different modes of nuclear excitations [9–11]. Selection rules in M1 transitions can also be used to probe symmetries and quantum numbers. One such symmetry is seniority (essentially the number of unpaired nucleons), which is known to be an approximate quantum number for identical nucleons in a single shell [12,13] but strongly broken in nuclei with neutrons *and* protons in the valence shell.

The strong spin-orbit coupling in the nucleus, a decisive ingredient for determining nuclear shell structure, leads to a splitting of orbits with $j = \ell + 1/2$ and $j = \ell - 1/2$. Among the various gaps so created, the one at $Z = 50$ is unique since it is the only one with adjacent spin-orbit partner orbits. The measured magnetic moments of odd-mass Sb [14] and In [15] deviate from their Schmidt limits (in an opposite fashion), as can be understood from core polarization and meson exchange, and accounted for by a renormalization of the M1 operator with the inclusion of a tensor term [6,7]. The evolution of the magnetic moments with N [16] is presumably due to particle-core coupling [14,17] but why this variation occurs in Sb and not in In remains unclear.

In neutron-rich Sb and In isotopes, the valence proton particle and hole occupy well-isolated orbits, $g_{7/2}$ or $g_{9/2}$, respectively. These isotopes thus provide a unique possibility to study the role of the individual magnetic properties of a valence particle/hole in spin-orbit partner orbits in M1 transitions. Additionally, the characterization of excited states of these isotopes will allow

* Corresponding author.
E-mail address: navin@ganil.fr (A. Navin).

http://dx.doi.org/10.1016/j.physletb.2015.11.077

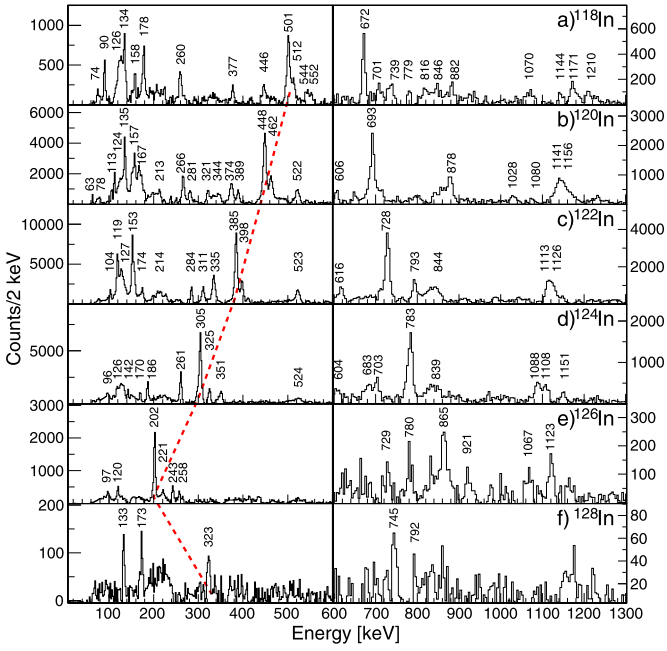

Fig. 1. (Color online.) A- and Z-identified Doppler-corrected γ-ray spectra for the odd–odd $^{118-128}$In isotopes (for energies greater than 600 keV the binning is doubled). A smooth background is subtracted from these spectra. The dashed line connects the most populated transition for each isotope, corresponding to the decay of the lowest populated excited state.

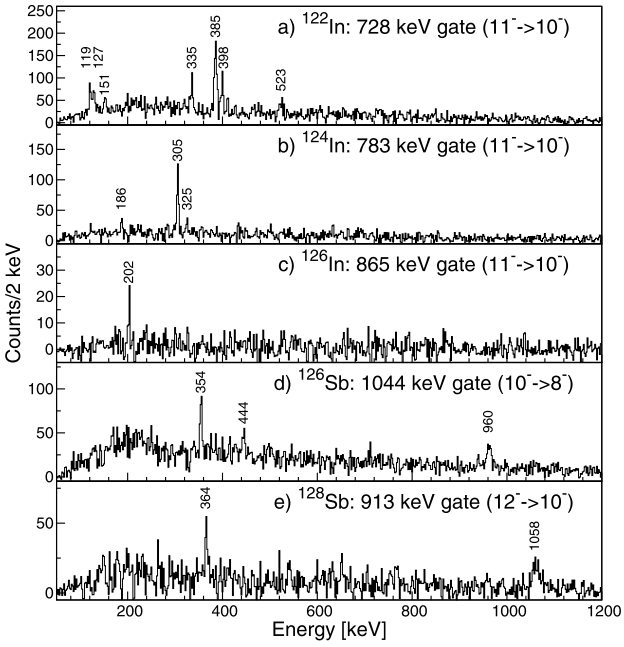

Fig. 2. A- and Z-identified Doppler-corrected γ-ray coincidence spectra for the ^{122,124,126}In isotopes (a–c) and ^{126,128}Sb isotopes (d–e).

us to address the questions whether the particle/hole nature of the proton influences the structural evolution with N and to what extent the presence of one single valence proton destroys the seniority symmetry of the neutrons. With the above motivation, we report in this letter on electromagnetic transitions, deduced from prompt γ spectroscopy of isotopically identified Sb and In isotopes with $N = 73, 75, 77$ produced in fission at an energy around the Coulomb barrier.

Odd-mass Sb and In isotopes have been investigated by isomer decay and in-beam spectroscopy [18–21]. Odd–odd isotopes have only been studied by β-decay [22–28] and the spectroscopy of their high-spin states in the vicinity of $N \lesssim 80$ is unknown. Excited states in nuclei far from stability have become accessible by means of radioactive-ion beams while those at high angular momentum have been studied using the combination of large γ-ray arrays with stable beams. More recently, the increased sensitivity of isotopic identification of fission fragments at energies around the Coulomb barrier, using a large-acceptance spectrometer coupled with an efficient γ-ray detector array, have allowed the study of nuclei at the extremes of both spin and isospin [29,30].

The measurements were made at GANIL using the magnetic spectrometer VAMOS++ [31,32] in coincidence with the γ-ray detector array EXOGAM [33]. Fragments from fusion–fission and transfer-induced fission were produced in collisions of ^{238}U, at an energy of 1.29 GeV, with a 10 µm-thick Be target. The typical intensity of the beam was 10^9 particles/s. The time-of-flight and the positions of incoming ions, along with the known ion optical properties of VAMOS++, were used to obtain on an event-by-event basis the magnetic rigidity Bρ, the velocity vector of the fission fragment $\mathbf{V}_{\mathrm{FF}}$, and the mass-over-charge A/q. The Z identification of the fission fragment was obtained from the correlation of the energy loss and the total energy. The energy of γ rays emitted by the nuclei was transformed to the rest frame by combining the measured direction of the γ-ray (using the segmentation of EXOGAM) and $\mathbf{V}_{\mathrm{FF}}$. Further details of the experimental method can be found in Refs. [29,30].

The isotopically identified γ-ray spectra of the even-mass $^{124-128}$Sb and $^{118-128}$In were measured. Figure 1 shows the spectra for the most exotic isotones measured in this work. All reported γ-ray transitions are observed for the first time. The dashed line indicates the evolution, as a function of N, of the energy difference between the two lowest populated levels. It smoothly decreases with increasing N; at $N = 79$ the trend reverses (the 323 keV transition is the most intense) implying a change in structure. In the following discussion we limit ourselves to the most neutron-rich isotopes of Sb and In studied here. Figure 2 shows the γ–γ coincidence spectra for the nuclei where it was possible. The derived partial level schemes for $N = 73, 75, 77$, obtained using γ–γ coincidences and relative intensities, are shown in Fig. 3.

The fission process favors the population of yrast states and the present experimental setup is sensitive only to states with lifetimes shorter than ∼2 ns (as states with larger lifetimes decay far from the Compton suppressed array). Therefore, all $\Delta J = 2$ transitions can be assumed E2 as any other multipolarity leads to levels that are too long-lived to be detected. Since crossover transitions are observed, $\Delta J = 1$ is adopted in the sequence of adjacent levels. The corresponding transitions are assumed to be M1, which are strongly favored over E2 for low-energy γ rays. It is unlikely that the $\Delta J = 1$ sequences are E1 transitions, hence the concerned levels can be assigned the same parity. The width of the arrows in Fig. 3 represents the branching ratio, normalized to the same decay probability for each level, with M1 (E2) transitions in red (blue). The ratios of reduced transition probabilities $B(\mathrm{M1})/B(\mathrm{E2})$, obtained from the measured branching ratios, and the γ-ray energies are also shown. What stands out from Fig. 3 is: (i) the unexpectedly different decay pattern, with a dominance of E2 transitions in Sb and of M1 transitions in In; (ii) a strong variation (which we conjecture to be a staggering) with increasing spin of $B(\mathrm{M1})/B(\mathrm{E2})$ ratios in the In isotopes; (iii) a smooth increase for Sb and decrease for In, with neutron number, of the energy difference between the two lowest states. These observations are interpreted below.

The shell model in the full relevant single-particle space leads to matrices of very large dimension. Calculations are therefore carried out in a restricted single-particle space consisting of the neu-

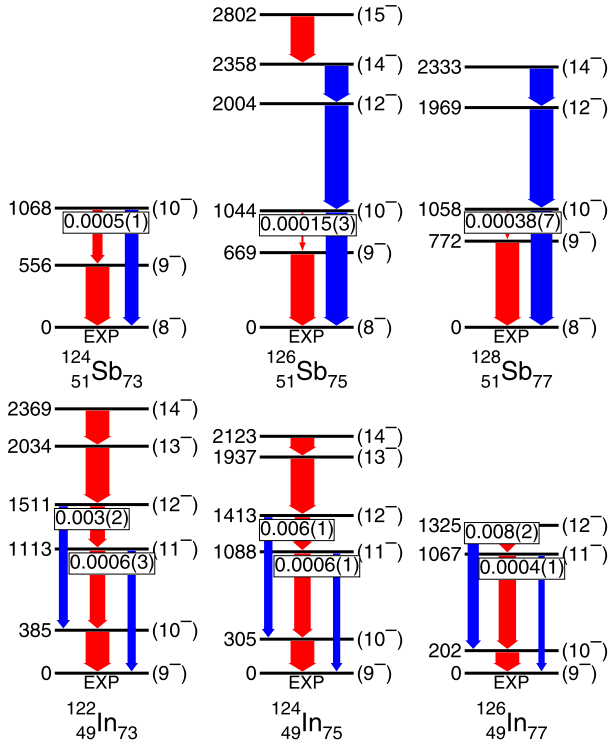

Fig. 3. (Color online.) Partial level schemes of the Sb and In isotopes built on the yrast low-energy high-spin states proposed in this work. Excitation energies (in keV) are relative to the 8^- (Sb) or 9^- (In) level. Transitions in red (blue) are M1 (E2). The width of the arrows represents the branching ratio, normalized to the same decay probability for each level. Also shown are the deduced $B(\mathrm{M1})/B(\mathrm{E2})$ ratios.

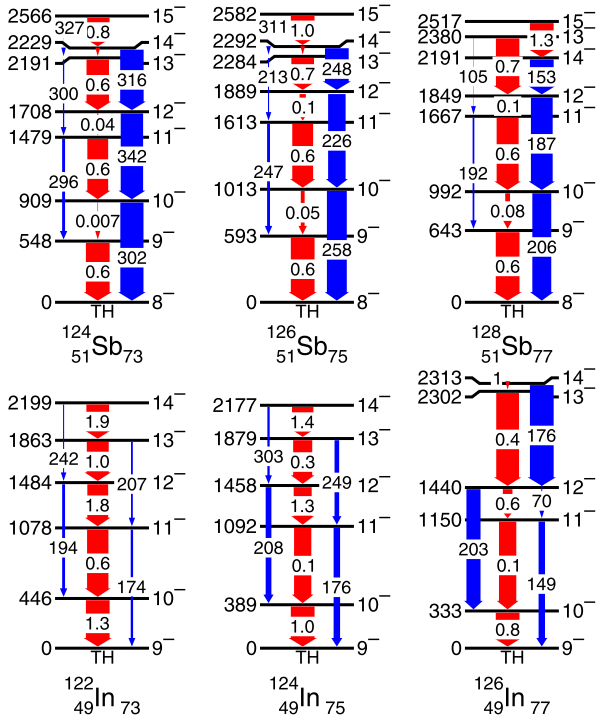

Fig. 4. (Color online.) Same as Fig. 3 for the full shell-model calculation (see text). The numbers on the arrows are the $B(\mathrm{M1})$ or $B(\mathrm{E2})$ values, in units of μ_N^2 and $e^2\mathrm{fm}^4$, respectively. To compare with the $B(\mathrm{M1})/B(\mathrm{E2})$ ratios quoted in Fig. 3, the $B(\mathrm{M1})$ value should be divided by the $B(\mathrm{E2})$ value of the transition starting from the same level.

tron (ν) $d_{3/2}$, $s_{1/2}$, $h_{11/2}$ orbits, and the proton (π) $g_{9/2}$, $p_{1/2}$, $g_{7/2}$ orbits near the Fermi surface. The interaction used is derived starting from the CD Bonn potential (jj45pn and jj55pn [34]) and calculations are performed with the codes NATHAN [35] and OXBASH [36]. The diagonal matrix elements for the neutrons are adjusted to account for missing correlations in the restricted model space. Effective charges of $e_\nu = 0.9$ and $e_\pi = 1.8$ are chosen so as to reproduce the measured $B(\mathrm{E2})$ values in the Sn and Te isotopes [37]. The orbital and spin parts of the M1 operator are taken as suggested by a microscopic calculation [7,14] and no tensor term is included (see below). Calculated low-spin levels are omitted from the spectrum and only the yrast levels built on the lowest high-spin state (8^- in Sb and 9^- in In) are shown in Fig. 4 (the fission process favors the population of yrast states). Fogelberg et al. [38,39] reported low-lying low-spin positive-parity (like $1^+, 3^+, 5^+$) states in ^{122,124,126}In, not observed in the present work. The presence of the crossover transitions connecting the lowest states observed in the present work allows to rule out a change of the parity of the levels in the sequence. The longer lifetimes of the M2 and higher multipolarity transitions, are beyond the sensitivity of the present experiment ($\lesssim$2 ns). The energy differences between the proposed $E(9^-) - E(8^-)$ (Sb) and $E(10^-) - E(9^-)$ (In) states (Fig. 3) and also those for the higher-lying states, evolve smoothly as a function of N in good agreement with the calculations (Fig. 4). The calculations for the In isotopes show that the $B(\mathrm{M1})$ values are generally large, $\sim$1 μ_N^2, and the $B(\mathrm{E2})$ values amount to $\sim$200 $e^2\mathrm{fm}^4$. In the Sb isotopes the $B(\mathrm{M1})$ values are smaller while $B(\mathrm{E2})$ values are larger than in In. The calculated $B(\mathrm{M1})$ values also show a staggering as a function of spin [related to observation (ii)]. The good agreement of the calculations with the observations constitutes the basis of the tentative spin-parity assignments and thus the M1 or E2 character of the relevant transitions in Fig. 3. Fogelberg et al. [39] measured the β-decay of the high-spin states in ^{120,122,124,126,128}In and tentatively suggested a J^π of 8^- for these states. The calculations predict the 8^- state to be the lowest in the lighter In ($A \leq 120$) isotopes, in ^{122}In it is close in energy to the 9^- state whereas in ^{124}In it lies close to the 10^- state and in ^{126}In it is $\sim$500 keV above the 10^-. If the lowest state is assumed to be 8^-, the corresponding sequence for the excited states $8^-, 9^-, 10^-$ would lead to a cascade of strong M1 transitions, without showing a staggering in $B(\mathrm{M1})/B(\mathrm{E2})$ ratios (as observed), since these states belong to the same multiplet.

A deeper insight into the three features seen in the data (and their ramifications) can be obtained from a simplified version of the above shell-model calculation where the observed low-energy, negative-parity states are considered to arise from a proton particle $j_\pi = g_{7/2}$ (Sb) or a proton hole $j_\pi^{-1} = g_{9/2}^{-1}$ (In) coupled to n_ν neutrons in $j_\nu = h_{11/2}$. The observed dominance of E2 transitions in Sb and of M1 transitions in In [observation (i)] can be explained as follows: if neutrons and protons are confined to specific orbits j_ν and j_π, the M1 matrix elements are proportional to the difference of g factors, $g(j_\nu) - g(j_\pi)$. The calculated effective M1 operator [7] for a g ($\ell = 4$) proton in this mass region [14] has $g(\pi g_{7/2}) = 0.84$ and $g(\pi g_{9/2}) = 1.43$. These compare well with the measured values $g(7/2_1^+) \approx 0.71$–0.86 in odd-mass Sb (depends on N) and $g(9/2_1^+) \approx 1.22$ in odd-mass In [16]. The corrections to the free M1 operator (which do not include effects from $\lambda^\pi \neq 1^+$ core polarization [17] nor two-body terms [40]) mainly concern the orbital (+14%) and the spin parts (−35%), as the tensor term contributes only 3% of the final result. No effective M1 operator is known for an h ($\ell = 5$) neutron in this mass region. Assuming the same spin quenching (−35%) for neutrons and protons, one finds $g(\nu h_{11/2}) = -0.23$, to be compared with the measured value $g(11/2_1^-) \approx -0.25$ in odd-mass Sn [16]. The g factors thus

determined lead to $B(\mathrm{M1})$ values that are ∼2 times larger in In than in Sb, as observed in Fig. 4.

The results of the simplified shell model can be further interpreted if a seniority (or broken-pair) classification is adopted for the neutrons. The interaction between the neutrons has seniority as an approximate symmetry, resulting in a spectrum that, for an odd number of neutrons in $\nu h_{11/2}$, has a ground state with seniority $\upsilon_\nu = 1$ and angular momentum $J_\nu = 11/2$ (no broken pair), and excited states with $\upsilon_\nu = 3$ or 5 (one or two broken pairs). It can be shown (based on first-order perturbation theory) that a state with n_ν neutrons with seniority υ_ν in the orbit j_ν and n_π protons with seniority υ_π in the orbit j_π is shifted in energy by the neutron–proton (np) interaction by an amount $\Delta E_{\nu\pi}$,

$$\Delta E_{\nu\pi} = n_\nu n_\pi \bar{V}_{j_\nu j_\pi} + \upsilon_\nu \upsilon_\pi \frac{1}{2}\left(V^{\alpha_\nu \alpha_\pi J}_{j_\nu j_\pi} + V^{\alpha_\nu \alpha_\pi J}_{j_\nu j_\pi^{-1}}\right) + f_\nu f_\pi \upsilon_\nu \upsilon_\pi \left[\frac{1}{2}\left(V^{\alpha_\nu \alpha_\pi J}_{j_\nu j_\pi} - V^{\alpha_\nu \alpha_\pi J}_{j_\nu j_\pi^{-1}}\right) - \bar{V}_{j_\nu j_\pi}\right], \quad (1)$$

where f_ρ ($\rho = \nu$ or π) is related to the fractional filling of the orbits, $f_\rho = 2(n_\rho - \upsilon_\rho)/(2j_\rho + 1 - 2\upsilon_\rho) - 1$. Three linear combinations of the np interaction matrix elements $V^J_{j_\nu j_\pi}$ occur, namely the monopole average $\bar{V}_{j_\nu j_\pi} \equiv \sum_J [J] V^J_{j_\nu j_\pi}/([j_\nu][j_\pi])$ and the sums

$$V^{\alpha_\nu \alpha_\pi J}_{j_\nu j_\pi} \equiv [J_\nu][J_\pi] \sum_{J'} [J'] V^{J'}_{j_\nu j_\pi} \sum_{\upsilon'_\nu J'_\nu} \sum_{\upsilon'_\pi J'_\pi} \times \left(c^{\upsilon'_\nu J'_\nu}_{\upsilon_\nu \upsilon_\nu J_\nu} c^{\upsilon'_\pi J'_\pi}_{\upsilon_\pi \upsilon_\pi J_\pi}\right)^2 \begin{bmatrix} j_\nu & j_\pi & J_\pi & J_\nu \\ J' & J'_\pi & J & J'_\nu \\ j_\nu & j_\pi & J_\pi & J_\nu \end{bmatrix}, \quad (2)$$

and

$$V^{\alpha_\nu \alpha_\pi J}_{j_\nu j_\pi^{-1}} \equiv -[J_\nu][J_\pi] \sum_{J'} [J'] V^{J'}_{j_\nu j_\pi} \sum_{\upsilon'_\nu J'_\nu} \sum_{\upsilon'_\pi J'_\pi} \times \left(c^{\upsilon'_\nu J'_\nu}_{\upsilon_\nu \upsilon_\nu J_\nu} c^{\upsilon'_\pi J'_\pi}_{\upsilon_\pi \upsilon_\pi J_\pi}\right)^2 \begin{Bmatrix} j_\nu & j_\pi & J_\pi & J_\nu \\ J' & J'_\pi & J & J'_\nu \\ j_\nu & j_\pi & J_\pi & J_\nu \end{Bmatrix}, \quad (3)$$

where $[x] \equiv 2x + 1$, α_ρ stands for $\upsilon_\rho J_\rho$, $c^{\upsilon' J'}_{n\upsilon J}$ is a coefficient of fractional parentage [12], $c^{\upsilon' J'}_{n\upsilon J} \equiv [j^{n-1}(\upsilon' J') J | \} j^n \upsilon J]$, and the symbol in curly (square) brackets is a $12j$ coefficient of the first (second) kind [41]. Equations (2) and (3) are the generalization to n nucleons of the particle-hole theorem proven in 1956 by Pandya for $n = 2$ [42].

Equation (1), with np matrix elements $V^J_{j_\nu j_\pi}$ taken from an empirical analysis [43] or, as is done here, from the full shell-model calculation, is used to elucidate the evolution of states with neutron number. Fig. 5 shows the diagonal interaction energies $\Delta E_{\nu\pi}$ for the $\upsilon_\nu = 1$, $J_\nu = 11/2$ (blue dashed line) and the $\upsilon_\nu = 3$, $J_\nu = 9/2$ (red dash-dotted line) neutron configurations for the 8^- (Sb) or 9^- (In) state, as a function of the number of neutrons n_ν in $\nu h_{11/2}$. A crossing of the $\upsilon_\nu = 1$ and $\upsilon_\nu = 3$ configurations (indicated by the arrows) occurs for both Sb and In. This is in contrast to the evolution of the 9^- (Sb) or 10^- (In) state (not shown) where the $\upsilon_\nu = 1$ configuration is always found to be lowest in energy for all n_ν.

Fig. 5 also shows the evolution with n_ν of the relative energy of the two same states after diagonalization (black solid line). The energy differences $E(9^-) - E(8^-)$ (Sb) and $E(10^-) - E(9^-)$ (In) can be seen to vary smoothly for most values of n_ν, increasing

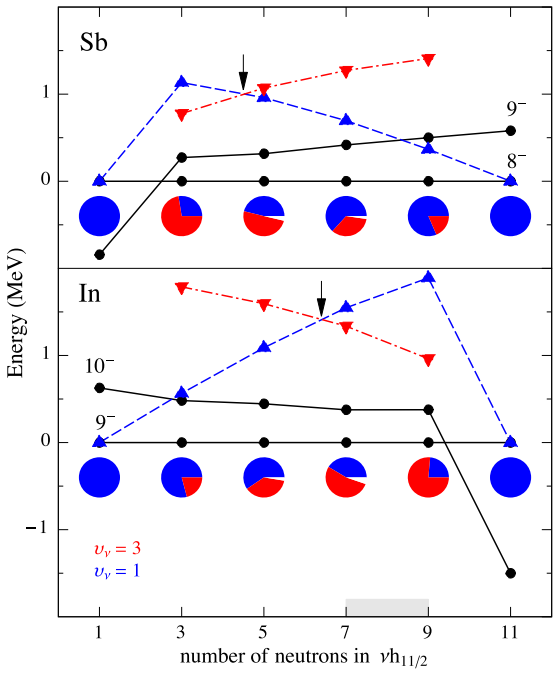

Fig. 5. (Color online.) Evolution of the relative energy of two high-spin states in odd–odd Sb and In isotopes, as predicted by a simplified shell-model calculation. The blue triangles (dashed line) and red triangles (dash-dotted line) are diagonal interaction energies $\Delta E_{\nu\pi}$ for the 8^- (Sb) or 9^- (In) state arising from a $\upsilon_\nu = 1$, $J_\nu = 11/2$ and a $\upsilon_\nu = 3$, $J_\nu = 9/2$ neutron configuration, respectively. The arrows indicate the crossing of configurations. The black dots (solid line) are obtained after diagonalization. The pie charts indicate the squares of the amplitudes (after mixing) of the $\upsilon_\nu = 1$, 3, and 5 components in blue, red, and white, respectively, for the 8^- (Sb) or 9^- (In) state. The gray area corresponds to the occupancies of $\nu h_{11/2}$ relevant for the isotopes studied here.

with n_ν in Sb and decreasing in In, as seen experimentally [observation (iii)] and in the full shell-model calculation. Also shown in Fig. 5 (as pie charts) are the squares of the amplitudes of the $\upsilon_\nu = 1$, 3, and 5 components of the wave function (after mixing) of the lowest 8^- (Sb) or 9^- (In) state. The reversal of seniorities is reflected in the pie charts. Additionally, Fig. 5 reveals the particle-hole symmetry as a similarity between the properties of an Sb isotope with n_ν neutrons and those of an In isotope with $12 - n_\nu$ neutrons. This generic behavior arises due to the 'Pandya' structure of Eq. (1) (reminiscent of the corresponding expression in terms of quasi-particles [44]).

The surprising and new feature revealed by our study is that the natural seniority ordering is easily broken. For the isotopes of interest here, with $7 \lesssim n_\nu \lesssim 9$ (occupancies of $\nu h_{11/2}$ as obtained in the full shell-model calculation), the seniority inversion occurs in In, the $\upsilon_\nu = 3$ configuration being lower in energy and the dominant component of the wave function. The feature of favoring energetically the state with one broken pair over that with no broken pairs is due to the interaction of a *single* proton with the neutrons. The character of the proton (*i.e.*, whether it is a particle or a hole) is of crucial importance in this mechanism. The interplay of like-nucleon pairing and neutron–proton interaction has been the topic of previous studies. For example, odd–even staggering effects of binding energies [45] depend on this interplay and, in particular, on the character (*i.e.* particle or hole) of the odd nucleon [46]. The present interpretation confirms indeed the importance of this character in the breaking of seniority.

In summary, the measured electromagnetic decay of neutron-rich odd–odd Sb and In isotopes is found to be strikingly different, and can be explained from the magnetic moment of a proton in spin-orbit partner orbits. The work highlights the important role

of a single proton (particle or hole) in the mixing of the seniority quantum number, leading to the dominance of the higher-seniority configuration in the In isotopes. This result is found to be independent of the interaction and demonstrates the importance of the neutron–proton interaction over the like-nucleon pairing interaction in these nuclei far from stability. This study calls for systematic measurements of lifetimes and spectroscopic factors in this region of the nuclear chart. Apart from their intrinsic interest as regards the evolution of nuclear structure far from stability, they could provide inputs for a deeper understanding of the components of the effective M1 operator.

Acknowledgements

We thank S. Bhattacharyya and C. Schmitt for help in various aspects of data collection, analysis and many useful discussions. We acknowledge the important technical contributions of J. Goupil, G. Fremont, L. Ménager, J. Ropert, C. Spitaels, and the GANIL accelerator staff. We also thank B.A. Brown for providing the jj55pna and jj45pna interaction files and V. Zelevinsky for very useful insights for improving the manuscript. S.B. acknowledges financial support for her stay at GANIL through the LIA France-India agreement.

References

[1] K. Heyde, P. von Neumann-Cosel, A. Richter, Rev. Mod. Phys. 82 (3) (2010) 2365–2419, http://dx.doi.org/10.1103/RevModPhys.82.2365.
[2] T. Schmidt, Z. Phys. 106 (5–6) (1937) 358–361, http://dx.doi.org/10.1007/BF01338744.
[3] H. Miyazawa, Prog. Theor. Phys. 6 (5) (1951) 801–814, http://dx.doi.org/10.1143/ptp/6.5.801.
[4] R.J. Blin-Stoyle, Proc. Phys. Soc. A 66 (12) (1953) 1158–1161, http://dx.doi.org/10.1088/0370-1298/66/12/312.
[5] A. Arima, H. Horie, Prog. Theor. Phys. 12 (5) (1954) 623–641, http://dx.doi.org/10.1143/PTP.12.623.
[6] A. Arima, et al., Adv. Nucl. Phys. 18 (1987) 1–106.
[7] I. Towner, Phys. Rep. 155 (5) (1987) 263–377, http://dx.doi.org/10.1016/0370-1573(87)90138-4.
[8] J. Li, et al., Phys. Rev. C 88 (6) (2013) 064307, http://dx.doi.org/10.1103/PhysRevC.88.064307.
[9] D. Bohle, et al., Phys. Lett. B 148 (4–5) (1984) 260–264, http://dx.doi.org/10.1016/0370-2693(84)90084-4.
[10] S. Frauendorf, Rev. Mod. Phys. 73 (2) (2001) 463–514, http://dx.doi.org/10.1103/RevModPhys.73.463.
[11] H. Hübel, Prog. Part. Nucl. Phys. 54 (1) (2005) 1–69, http://dx.doi.org/10.1016/j.ppnp.2004.06.002.
[12] I.I. Talmi, Simple Models of Complex Nuclei: The Shell Model and Interacting Boson Model, Harwood Academic Publishers, Chur, Switzerland, Langhorne, PA, USA, 1993.
[13] P. Van Isacker, S. Heinze, Ann. Phys. 349 (2014) 73–99, http://dx.doi.org/10.1016/j.aop.2014.06.011.
[14] N. Stone, et al., Phys. Rev. Lett. 78 (5) (1997) 820–823, http://dx.doi.org/10.1103/PhysRevLett.78.820.
[15] J. Eberz, et al., Nucl. Phys. A 464 (1) (1987) 9–28, http://dx.doi.org/10.1016/0375-9474(87)90419-2.
[16] N. Stone, At. Data Nucl. Data Tables 90 (1) (2005) 75–176, http://dx.doi.org/10.1016/j.adt.2005.04.001.
[17] I. Hamamoto, Phys. Lett. B 61 (4) (1976) 343–346, http://dx.doi.org/10.1016/0370-2693(76)90583-9.
[18] M. Górska, et al., Phys. Lett. B 672 (4–5) (2009) 313–316, http://dx.doi.org/10.1016/j.physletb.2009.01.027.
[19] R. Lucas, et al., Eur. Phys. J. A 15 (3) (2002) 315–323, http://dx.doi.org/10.1140/epja/i2002-10042-8.
[20] M.G. Porquet, et al., Eur. Phys. J. A 24 (1) (2005) 39–49, http://dx.doi.org/10.1140/epja/i2004-10119-4.
[21] M.-G. Porquet, et al., Eur. Phys. J. A 20 (2) (2004) 245–250, http://dx.doi.org/10.1140/epja/i2003-10161-8.
[22] D.O. Elliott, et al., Z. Phys. 269 (2) (1974) 89–95, http://dx.doi.org/10.1007/BF01669048.
[23] H.A. Smith, et al., Phys. Rev. C 13 (1) (1976) 387–398, http://dx.doi.org/10.1103/PhysRevC.13.387.
[24] L.L. Nunnelley, W. Loveland, Phys. Rev. C 13 (5) (1976) 2017–2023, http://dx.doi.org/10.1103/PhysRevC.13.2017.
[25] C. Li, et al., Nucl. Phys. A 892 (2012) 34–42, http://dx.doi.org/10.1016/j.nuclphysa.2012.07.013.
[26] Ø. Scheidemann, E. Hagebø, J. Inorg. Nucl. Chem. 35 (9) (1973) 3055–3059, http://dx.doi.org/10.1016/0022-1902(73)80002-8.
[27] H. Göktürk, et al., Z. Phys. A 324 (1) (1986) 117–118, http://dx.doi.org/10.1007/BF01290762.
[28] A. Scherillo, et al., Phys. Rev. C 70 (5) (2004) 054318, http://dx.doi.org/10.1103/PhysRevC.70.054318.
[29] A. Navin, M. Rejmund, Gamma-ray spectroscopy of neutron-rich fission fragments, in: McGraw–Hill Yearbook of Science & Technology, 2014, p. 137.
[30] A. Navin, et al., Phys. Lett. B 728 (1) (2014) 136–140, http://dx.doi.org/10.1016/j.physletb.2013.11.024.
[31] S. Pullanhiotan, et al., Nucl. Instrum. Methods Phys. Res., Sect. A 593 (3) (2008) 343–352, http://dx.doi.org/10.1016/j.nima.2008.05.003.
[32] M. Rejmund, et al., Nucl. Instrum. Methods Phys. Res., Sect. A 646 (1) (2011) 184–191, http://dx.doi.org/10.1016/j.nima.2011.05.007.
[33] J. Simpson, et al., Acta Phys. Hung., Heavy Ion Phys. 11 (1–2) (2000) 159–188.
[34] M. Hjorth-Jensen, T.T.S. Kuo, E. Osnes, Phys. Rep. 261 (3–4) (1995) 125–270, http://dx.doi.org/10.1016/0370-1573(95)00012-6.
[35] E. Caurier, et al., Phys. Rev. C 59 (4) (1999) 2033–2039, http://dx.doi.org/10.1103/PhysRevC.59.2033.
[36] B.A. Brown, et al., MSI-NSCL Report No. 524, 1985.
[37] D. Radford, et al., Nucl. Phys. A 746 (2004) 83–89, http://dx.doi.org/10.1016/j.nuclphysa.2004.09.056.
[38] B. Fogelberg, T. Nagarajan, B. Grapengiesser, Nucl. Phys. A 230 (2) (1974) 214–220, http://dx.doi.org/10.1016/0375-9474(74)90303-0.
[39] B. Fogelberg, P. Carlé, Nucl. Phys. A 323 (2–3) (1979) 205–252, http://dx.doi.org/10.1016/0375-9474(79)90108-8.
[40] M. Nomura, Phys. Lett. B 40 (5) (1972) 522–524, http://dx.doi.org/10.1016/0370-2693(72)90471-6.
[41] A.P. Yutsis, I.B. Levinson, V.V. Vanagas, Theory of angular momentum (matematicheskii apparat teorii momenta kolichestva dvizheniya), NASA TT F-98, 1962.
[42] S.P. Pandya, Phys. Rev. 103 (4) (1956) 956–957, http://dx.doi.org/10.1103/PhysRev.103.956.
[43] J.P. Schiffer, W.W. True, Rev. Mod. Phys. 48 (2) (1976) 191–217, http://dx.doi.org/10.1103/RevModPhys.48.191.
[44] J. Van Maldeghem, K. Heyde, J. Sau, Phys. Rev. C 32 (3) (1985) 1067–1075, http://dx.doi.org/10.1103/PhysRevC.32.1067.
[45] J. Hakala, et al., Phys. Rev. Lett. 109 (3) (2012) 032501, http://dx.doi.org/10.1103/PhysRevLett.109.032501.
[46] L. Coraggio, et al., Phys. Rev. C 88 (4) (2013) 041304, http://dx.doi.org/10.1103/PhysRevC.88.041304.